Assessment of Drought Effects on Forests using Non-Parametric Methods and Satellite Imagery

SIMON KÖNIG[1], JOHANNES SCHULTZ[1,2], OLENA DUBOVYK[1,3] & FRANK THONFELD[4,5]

Abstract: Temperate forests are a vital part of the natural environment and important for human existence. Yet, they are increasingly threatened by changing disturbance regimes, especially more severe droughts. Here, we combine Landsat and Sentinel-2 time series and use a kernel density estimation (KDE) to assess the baseline phenology of a mixed forest area in Germany. We compared this baseline to the forest's development during the drought year of 2018 and the following growing season of 2019. Our results show that parts of the examined forest were negatively impacted to an unprecedented degree. With the use of satellite remote sensing analyses and the KDE, we can assess the impact of drought on vegetation development without relying on parametric methods.

1 Introduction

Forests are a key component of the natural environment in tropical, temperate and boreal regions as well as a major foundation for human existence in these areas. Locally and regionally, they provide a variety of ecosystem services. This includes the provision of wood-related products, the filtering of water or regulation of climate as well as the potential for recreation and tourism. In Europe, forestry is among the most important economic sectors. Besides being biodiversity hosts, forests are an integral part of global land-atmosphere interactions (BONAN 2008). Temperate forests serve as major net carbon sinks. Contrasting tropical and boreal forests, the amount of carbon stored inside the temperate forest biome increased between 2000 and 2007 compared to the decade before (PAN et al. 2011), partly outweighing anthropogenic CO_2 emissions. Consequently, temperate forests play a key role in mitigating climate change.

Natural disturbances, such as windthrow, fires and insect outbreaks, are crucial for ecosystem functions and the dynamics of forests. As they change the composition, structure and function of forests, they contribute to their heterogeneity, facilitate biodiversity and stimulate succession, reorganization and renewal (SEIDL et al. 2017). During the last decades however, disturbance regimes have changed globally. For many regions, disturbances are increasingly prevalent and becoming more frequent and severe. This includes fires, insect outbreaks and droughts. So-called 'megadisturbances' (MILLAR & STEPHENSON 2015) are emerging, having the potential to increase

[1] Rheinische Friedrich-Wilhelms-Universität Bonn, Geographisches Institut, Meckenheimer Allee 166, D-53115 Bonn, E-Mail: [simonkoenig, odubovyk]@uni-bonn.de

[2] Ruhr-Universität Bochum, Geographisches Institut, Universitätsstraße 150, D-44801 Bochum, E-Mail: johannes.schultz@rub.de

[3] Rheinische Friedrich-Wilhelms-Universität Bonn, Zentrum für Fernerkundung der Landoberfläche, Genscherallee 3, D-53113 Bonn

[4] Deutsches Fernerkundungsdatenzentrum, Münchner Straße 20, 82234 Wessling, E-Mail: frank.thonfeld@dlr.de

[5] Julius-Maximilians-Universität Würzburg, Institut für Geographie und Geologie, Oswald-Külpe-Weg 86, D-97074 Würzburg

tree mortality to a level surpassing historical recordings and alter forests beyond their ecological resilience. Consequently, there are increasing rates of canopy mortality being observed across Europe's temperate forests (SENF et al. 2018). Many of these changes in disturbance regimes are attributed to climate change – SEIDL et al. (2017) state that temperature and water availability are the most important drivers of disturbances in the temperate forest biome. There is strong evidence that disturbance activity is going to increase with both warmer and wetter as well as warmer and drier climatic conditions; and that climate change will facilitate large-scale disturbance episodes across Europe's temperate forests (SENF & SEIDL 2018).

In this context, drought is an especially important disturbance agent. Climate observations and projections suggest that droughts are increasing in both more frequency and magnitude in the wake of a generally hotter climate in Europe. ALLEN et al. 2015 and MILLAR & STEPHENSON 2015 refer to these emerging, more severe droughts that are coupled with high temperature events as 'hotter droughts' or 'global-change-type droughts'. These affect forests both directly and indirectly. Their direct effects include the increase of evaporation and heat damage due to higher temperatures, with a simultaneous increase in water stress due to a lack of precipitation. Additionally, a generally warmer climate leads to less precipitation in the form of snow that serves as a water reservoir (MILLAR & STEPHENSON 2015). Indirectly, droughts increase the susceptibility of trees to other disturbances, especially pathogens, fires and insect outbreaks while facilitating the activity of insects and intensify the risk of fires – there is strong evidence that an increase in droughts also leads to increased fire and insect disturbances (ALLEN et al. 2015; SEIDL et al. 2017).

As an example event to assess drought effects on forests, we use the major drought that took place in large parts of Central, Northern, and Western Europe in the summer of 2018. The drought was characterized by considerable rainfall lacks, combined with exceptionally high temperatures, especially during June and July. Hence, this event can probably be characterized as one of the global-change-type droughts mentioned above. Summer temperatures in Germany were only exceeded by temperatures in 2003, and the lack of rainfall in some areas was unprecedented in the historical recordings (IMBERY et al. 2018). The drought had severe consequences for vegetation health and crop yield (REINERMANN et al. 2019) and especially forests, with widespread low remote sensing vegetation index values and a strongly reduced vegetation productivity. Increased tree mortality during 2018 and 2019 is also reported, but partly may also be attributed to legacy effects and not only the drought itself (BURAS et al. 2019).

Remote sensing has been a widely used tool to appraise the impacts of drought events on ecosystems for decades (AGHAKOUCHAK et al. 2015). However, the impacts of droughts on forests have often been underestimated (ALLEN et al. 2015) and there are various challenges to the remote sensing of these effects, including the choice of proper datasets with regards to resolution and coverage as well as the appropriate assessment method (ZHANG et al. 2013). It is feasible to compare the impacts of droughts or other disturbances to forest's typical phenology to get a sense of how severe it is. These comparisons however have often been based on parametric methods that may not actually well explain forest's phenological cycles (CHÁVEZ et al. 2019). Additionally, there is a need for approaches that allow a near-realtime monitoring of drought events (ALLEN et al. 2015) as well as working with multi-sensor data to be more resilient towards cloudy pixels (ZHANG et al. 2013). Furthermore, some drought effects exhibit delays and take place in the years following the drought events, so it is often sensible to consider a study period of multiple years.

Here, we try to meet these requirements by estimating the impact of the drought of 2018 in on a mixed forest in Germany. This is done in a non-parametric way that allows for the comparison to a baseline phenology. We use all data from the Landsat and Sentinel-2 sensors available since the year 2000 and compare the forests' development for the years 2018 and 2019 to their phenological baseline, computed using a kernel density estimation (KDE).

2 Data & Methods

2.1 Study Area

The proposed procedure of this study is tested for a mixed forest area in Germany: the *Kottenforst* area (Fig. 1a), located directly in the south west of the city of Bonn in the state of North-Rhine-Westphalia, is a cohesive forest area of about 40 km^2 size. Though there are a variety of tree species abundant, *Quercus robur L.* (Common oak), *Quercus petraea MATT.* (Sessile Oak), *Picea abies L.* (Norway Spruce) and *Fagus sylvatica L.* (European Beech) prevail in most areas (BOSCH 1997). The area is relatively humid, typically receiving around 650 mm of rainfall annually (WACHTER 2009). The forest is protected to a diverging degree. Namely, large areas are strictly protected, whereas some allow for forestry to some degree and contain plantations.

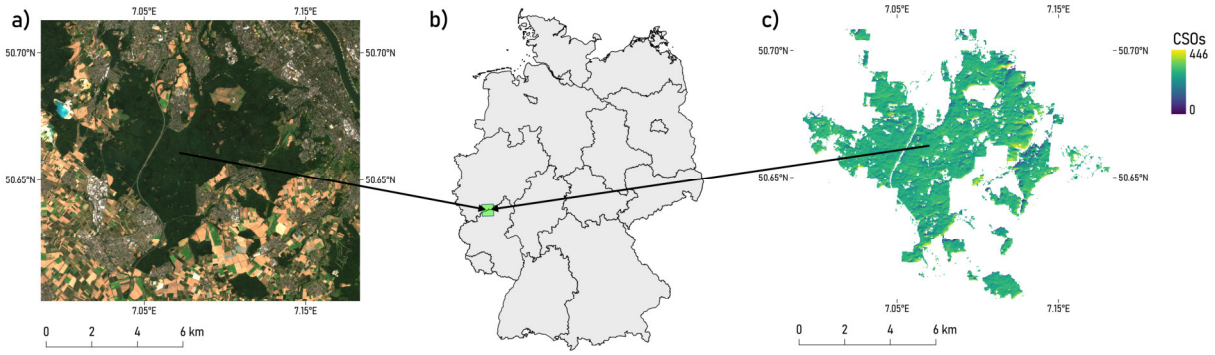

Figure 1: Study area Kottenforst. A cloud-free Sentinel-2 composite (a) and the position of the study area inside Germany are displayed (b). In b), the green box indicates the tile of the common Landsat/Sentinel-2 gridding system in which the area is located. c) displays the forest pixels of the area that did not experience a stand-replacing disturbance between 2000 and 2017 with the number of clear sky observations (CSOs), i.e. the number of pixels that were not contaminated by clouds, snow, aerosols etc. based on each image's quality flags.

2.2 Data

For this study, data from different moderate-resolution multispectral sensors were used. This includes Landsat TM, ETM+ and OLI as well as Sentinel-2 MSI imagery. With their similar spatial spectral characteristics, they can be used as a 'virtual constellation' (WULDER et al. 2015) whose data can be combined to create a denser time series and be more independent from cloud coverage. We regarded all available imagery of these sensors from January 01, 2000 to September 30, 2019. Data before the year 2000 was not included for two reasons: first, the shorter period reduced the prevalence of trends in the data and thus reduces their effect on the fitting of the baseline phenology. Second, we used secondary data to remove areas that are not suitable for this study whose data range however only includes the period since 2000. In total, we acquired 1823 images: 927 Landsat and 896 Sentinel-2 scenes.

2.3 Methods

The multi-sensor satellite imagery had to be properly radiometrically corrected to ensure a sensible inter-calibration between the sensors. Here, we used the *Framework for Operational Radiometric Correction for Environmental monitoring* (FORCE; FRANTZ 2019). FORCE can generate analysis-ready data (ARD) from both Sentinel-2 MSI as well as Landsat TM, ETM+ and OLI data by applying one consistent pre-processing scheme (FRANTZ et al. 2016). We applied the FORCE built-in topographic, atmospheric and BRDF corrections. Both Landsat and Sentinel-2 data were projected into one common, tiled grid to ease further processing; whereby Sentinel-2 was resampled to the 30 m resolution that matches the Landsat sensors. During processing, the FORCE software also created a variety of quality flags for each image, including a cloud and cloud shadow mask based on the *Fmask* algorithm (ZHU et al. 2015). However, the algorithm implemented in FORCE is adjusted for the lack of a thermal infrared band in the Sentinel-2 data – it considers parallax effects in the imagery to better detect clouds (FRANTZ et al. 2018). The output of the FORCE preprocessing steps was one consistent data cube of ARD at 30 m resolution, with cloudy and otherwise contaminated pixels being excluded and both Landsat and Sentinel-2 imagery projected into one common gridding system (FRANTZ 2019).

To ensure that only forest pixels were considered that did not experience any stand-replacing disturbance which would distort the fitting of the baseline, we applied one final preprocessing step. Using the global forest change data by HANSEN et al. (2013) implemented in Google Earth Engine (GEE; GORELICK et al., 2017), we generated a mask of all pixels that were classified as forest in 2000 and were not regarded as 'lost' until 2017. This mask was exported from GEE and applied to the ARD output of FORCE. The utilization of this procedure limited the suitable Landsat data to the period since 2000. From the resulting data we computed two multispectral indices to assess the drought effects: first, the Normalized Difference Vegetation Index (NDVI) as the most common remote sensing index that is sensible to plant health was regarded, which calculates as follows:

$$NDVI = \frac{NIR-Red}{NIR+Red} \quad (1)$$

where NIR corresponds to the near infrared and Red to the red band in the imagery. The second used index, the Normalized Difference Moisture Index (NDMI) is more sensitive to leaf water content and consequently especially suitable to detect the effects of droughts (cf. ZHANG et al. 2013). It is calculated similarly to the NDVI:

$$NDMI = \frac{NIR-SWIR1}{NIR+SWIR1} \quad (2)$$

where $SWIR1$ corresponds to the first shortwave infrared band of both Landsat and Sentinel-2. The NDVI and NDMI data were used as the input for the drought-related analysis itself, i.e. the fitting of a phenological baseline of the years 2000-2017 and the comparison of the drought year of 2018 and the follow-up year of 2019 to this baseline. The fitting of the phenological baseline is done with a non-parametric procedure by using a bivariate kernel density estimation (KDE). This approach was first introduced by CHÁVEZ et al. (2019) to assess insect defoliation in deciduous forests in South America based on MODIS Enhanced Vegetation Index (EVI) imagery. It was implemented into the npphen package (CHÁVEZ et al. 2017) for the R programming language (R CORE TEAM 2019) and modified for this study.

The procedure is graphically documented in Fig. 2 and consisted of five distinct steps: First, each pixel's NDVI/NDMI time series was divided into a baseline period – the years of 2000 to 2017 – and the target period in which the drought and its immediate aftermath took place – January 01, 2018 to September 30, 2019 (Fig. 2a). The dates of the baseline period where then converted to Day of Year (DOY) values, resulting in a transformed feature space where DOY is the independent

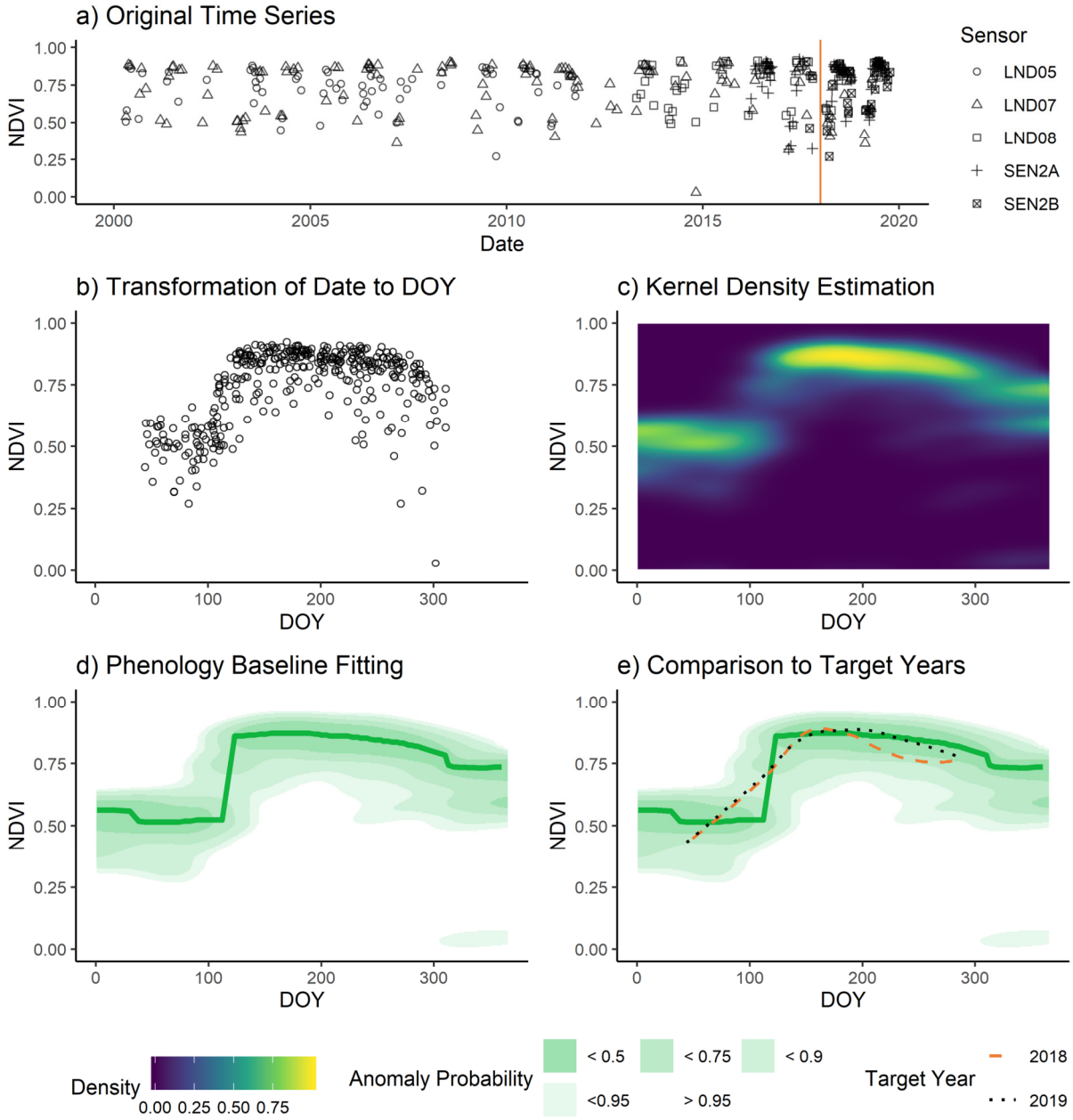

Figure 2: Analysis procedure exemplified for the NDVI values of one pixel in the Kottenforst area. The original time series (a) is divided into a baseline and a target period, as indicated by the orange line. The values of the baseline period are transformed into a DOY-NDVI feature space (b), for which a KDE is applied (c). From this KDE, the phenological baseline (dark green line) as well as the probability of an observation being an anomaly (light green shades) can be derived (d). Both can then be compared to the target year observations, likewise converted to DOY-NDVI values (e).

and NDVI or NDMI, respectively, is the dependent variable (Fig. 2b). Mathematically, the feature space can be described as $X_i = (DOY_i;\ IND_i)^T, i = 1, \ldots, n$ where IND is the respective remote sensing index (ESTAY & CHÁVEZ 2018). This feature space served as the input for the KDE. The goal of the KDE is now to approximate the probability density function $f(x)$:

$$\hat{f}(x; H) = \frac{1}{n}\sum_{i=1}^{n} K_H(x - X_i) \qquad (3)$$

where x corresponds to a generic point in the feature space X_i. K denotes the used kernel, which is a Gaussian kernel in this case (DUONG et al. 2019); and H is the estimated smoothing bandwidth that serves as an input for the kernel (WAND & JONES 1995, p. 91). The resulting density estimate (Fig. 2c) is standardized to sum 1 and consequently transformed into a 2-dimensional probability distribution, allowing for the derivation of confidence intervals around the most probable index value per DOY. This most probable index value forms the phenological baseline for each year (Fig. 2d). When the phenological baseline is compared to the observations of the target years (likewise converted to DOY-Index value pairs), these confidence intervals can be used to assess whether the observed values are actually a 'true' anomaly (Chávez et al., 2019). In addition to the difference in index values between baseline phenology and actual observations, the likelihood of these differences being an anomaly is an additional output (Fig. 2e). While the whole procedure is exemplified here for one pixel, it was applied to all forest pixels without stand-replacing disturbance between 2000 and 2017 in the Kottenforst area. Thereby, the raster-based function of the npphen package returns data cubes of the difference in index values between the fitted baseline and the observed values.

3 Results & Discussion

As there were two years being observed using two different vegetation health indices, a total of four data cubes were output. Fig. 3 illustrates the difference between baseline and observation for one example timestep of 2018 and one of 2019 for both indices. Fig. 4 depicts the complete vegetation development of 2018 and 2019 compared to the phenological baseline for one pixel.

As Fig. 3 depicts, the drought did indeed influence the two examined forests, not only in the drought year of 2018, but also during the following vegetation period in 2019. In the Kottenforst area, NDVI values did not differ much from their phenological baseline during the peak of the drought at the end of July (Fig. 3a) but were still lower typically. In terms of the NDMI, negative differences were not extreme, but still visible, indicating a reduced leaf water content (Fig. 3b). By mid-2019, NDVI values were restored to baseline values in most areas, even being higher than regular in some. Yet, there are several small patches with very high negative anomalies – the negative difference in NDVI values between baseline and observation typically amounted to 0.5 or greater (Fig. 3c). At the same time, during mid-June of 2019, NDMI values were lower for large parts of the forest, implying a longer-term consequence of the drought: a reduced leaf water content even if the NDVI values are regular or above in the consecutive growing season. This may possibly be caused by an ongoing lack of soil moisture.

As the example pixel marked in Fig. 3 is part of a Norway spruce plantation, it did not experience much yearly phenological variation during the reference period, as illustrated by the bold green lines in Fig. 4a and 4b. Yet there has been some general variability, indicated by the relatively

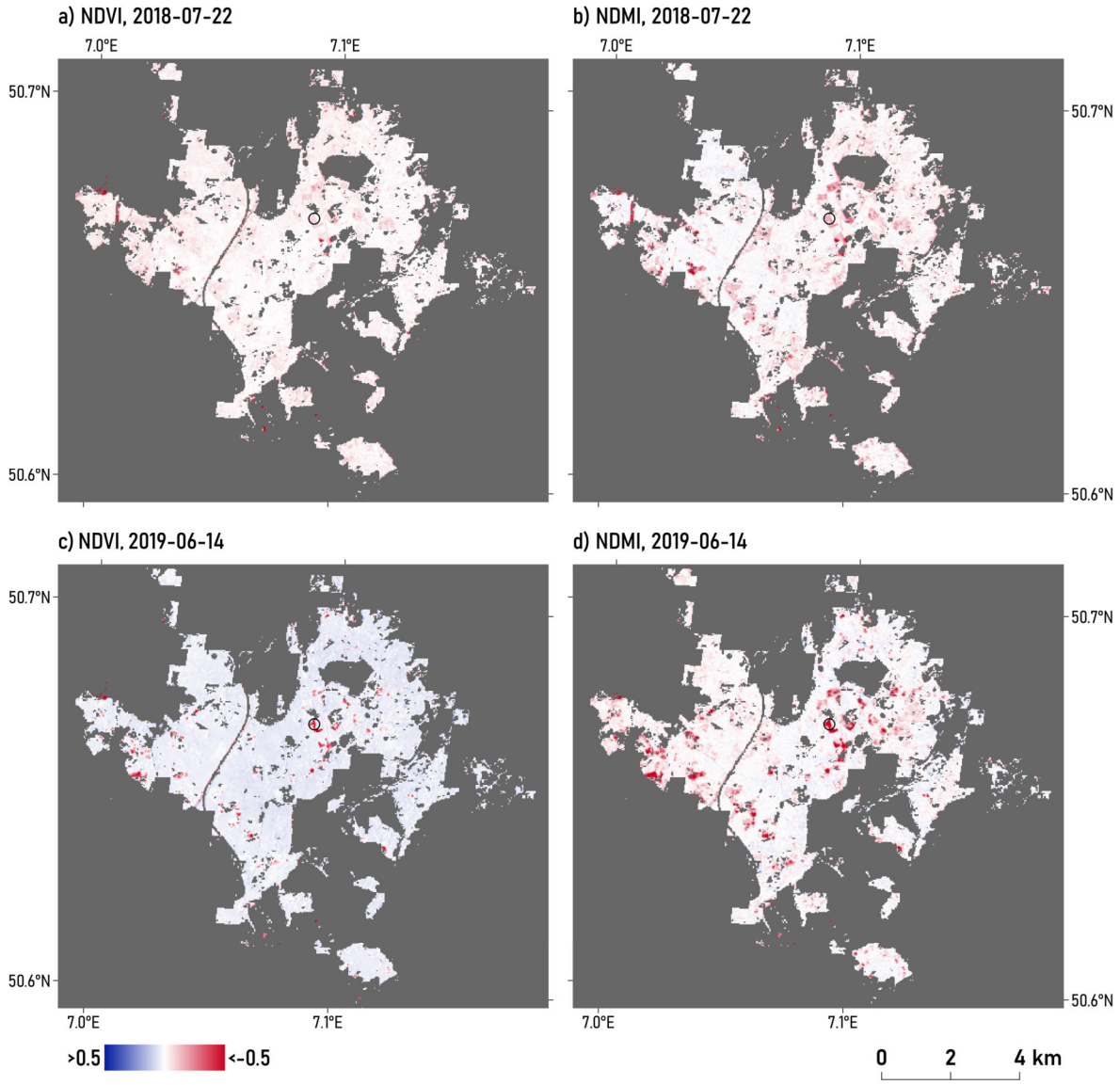

Figure 3: Example results of the Kottenforst area for one day in 2018 (a, b) and 2019 (c, d), both chosen due to low cloud coverage. NDVI (a, c) and NDMI (b, d) differences from the baseline are displayed for all available pixels. White indicates a difference of zero, blueish colors illustrate positive deviations, red indicates negative differences. Grey areas are either cloud-contaminated, not covered by forest or did experience a stand-replacing disturbance during the reference period. The black circle is centered around an example pixel (see Fig. 4).

wide confidence intervals, displayed as lighter green shades. NDVI and especially NDMI values for 2018 were below the baseline, especially during the second half of the year. In 2019, both indices diminished and the probability of the respective values being an anomaly is very high, with NDMI exceeding 0.95 in some parts of the year. The plantation suffered from water stress and bark beetle attacks in 2018 and was thus clear-cut in 2019, which likely explains these results.

The procedure applied here has both advantages and limitations. A strong advantage is its non-parametric nature. The approach neither relies on any thresholds nor predefined functions, e.g.

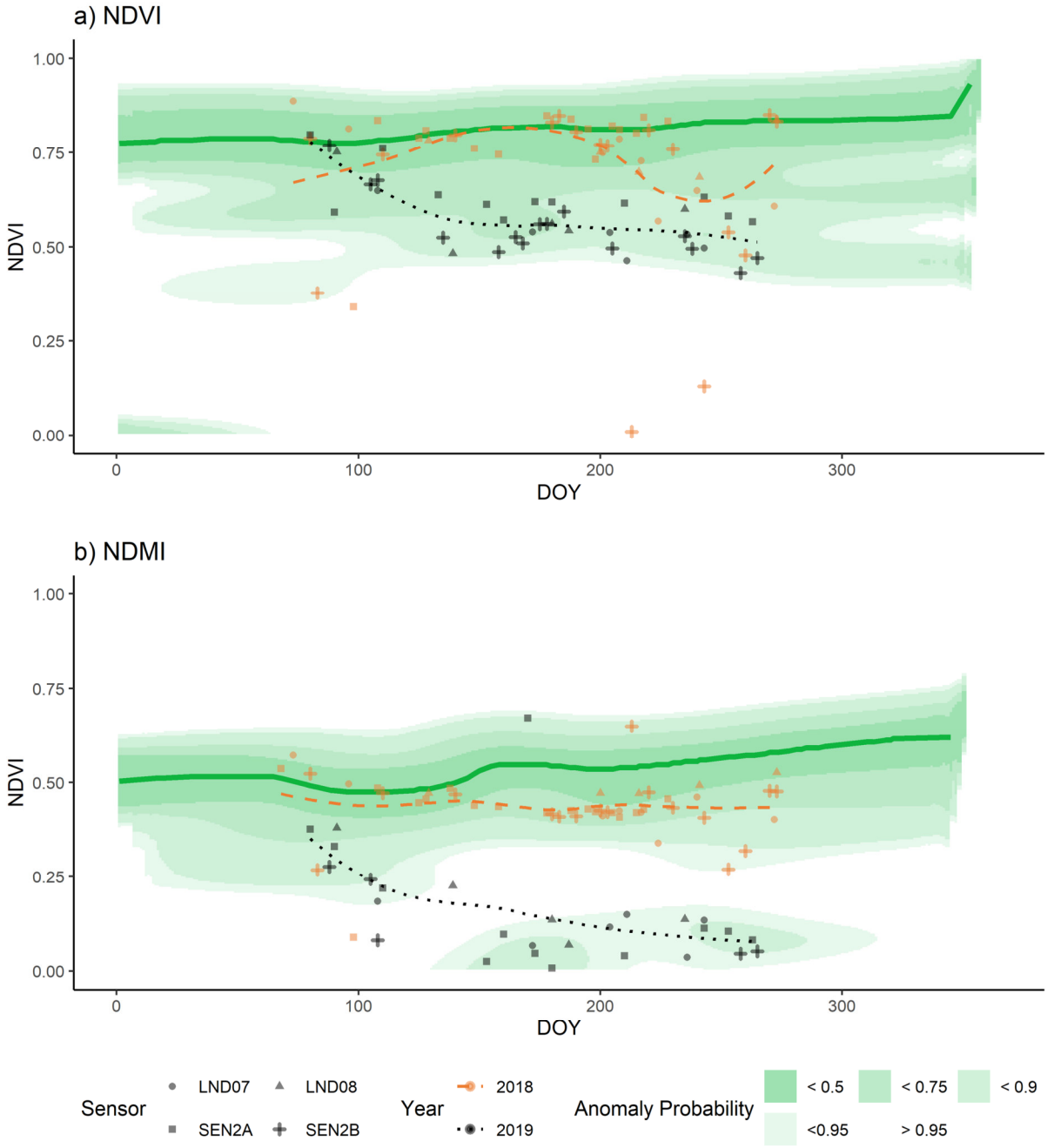

Figure 4: Phenological baseline in terms of NDVI (a) and NDMI (b) for the pixel indicated in Fig. 3. The bold green line is the baseline, the lighter shaded areas indicate the anomaly probability. Superimposed are the respective DOY-Index values for 2018 (orange) and 2019 (black) as points, the lines in the respective colors are smoothing splines that are fit using these points.

harmonic functions (ZHU et al. 2012) to represent seasonality. Instead, it uses the observed vegetation community and its dynamics itself (cf. ESTAY & CHÁVEZ 2018). The system is consequently easily applicable to different ecosystems. Beneficial is also its high robustness to missing and faulty values as well as outliers. This is visible in Fig. 4b where there apparently were

some outliers that caused the ribbons in the bottom center. These however had no influence on the fitted phenology baseline. In contrast to other methods that have similar targets, this procedure not only quantifies anomalies but also clarifies the degree of deviation from the regular phenology in terms of confidence intervals. This is highly important, especially if in the case of a drought event, management measures have to be planned and applied. Using the medium-resolution Landsat and Sentinel-2 sensors results in an increased spatial precision compared to coarser-resolution sensors like MODIS, while the combination of both leads to a temporal resolution that is still comparably high. Thus, the procedure meets several of the demands to forest drought impact assessments mentioned in the introduction.

Among the limitations of our approach is the fact that, while the alterations of vegetation development during a drought year can be assessed, there is no direct proof that these alterations were actually caused by the drought. Possible biases in this context include the interplays of drought with other disturbances and legacy effects of past influences of the forest (BURAS et al. 2019; SEIDL et al. 2017). Furthermore, outliers in the data, as exemplified by Fig. 4b, often may not influence the phenological baseline, but its confidence intervals. Including proper measures in our workflow to remove these outliers and compute more accurate confidence intervals would be a meaningful enhancement. An additional improvement may be the application and comparison of different remote sensing indices. Using the Vegetation Condition Index for example that scales each pixel's NDVI time series with its respective maximum and minimum and that is commonly applied in drought impact assessments (AGHAKOUCHAK et al. 2015; KOGAN 1990) or the Disturbance Index (HEALEY et al. 2005), commonly used in forest disturbance research, may further increase the validity of the results.

4 Conclusion

We applied a non-parametric procedure as well as multi-sensor multispectral satellite imagery to estimate the effects of droughts a mixed forest area in Germany. This study serves as a proof of concept and showed that the original idea of using a kernel density estimation and satellite imagery to analyze forest disturbances is feasible. It cannot only be performed for MODIS data with relatively coarse resolutions and uniform observation cycles (cf. CHÁVEZ et al. 2019), but is also transferrable to higher-resolution, multi-source data with variable spatial, spectral and temporal characteristics. While there are some issues and problems remaining, solving which would considerably improve the approach and resolve several pitfalls, the idea works well and may further be elaborated. Combining it with in-situ data could be a benefit, e.g. to compare the drought response of different tree species. The method may be not only for drought effects on forests, but also for other ecosystems as well as disturbances or other phenomena that require the comparison of a vegetation community's yearly development to their baseline phenology. The approach can complement other techniques that serve the same purpose and can technically be even used for operational monitoring, where the phenological baseline is updated if a season without a major disturbance takes place and each new satellite observation is compared to it. To summarize, the method can be highly beneficial to researchers and users that are concerned with investigating and monitoring the temperate forests of Europe where disturbance regimes, especially the prevalence of droughts, are changing rapidly.

5 References

AghaKouchak, A., Farahmand, A., Melton, F.S., Teixeira, J., Anderson, M.C., Wardlow, B.D. & Hain, C.R., 2015: Remote sensing of drought: Progress, challenges and opportunities. Reviews of Geophysics, **53**, 452–480.

Allen, C.D., Breshears, D.D. & McDowell, N.G., 2015: On underestimation of global vulnerability to tree mortality and forest die-off from hotter drought in the Anthropocene. Ecosphere, **6**, 129.

Bonan, G.B., 2008: Forests and Climate Change: Forcings, Feedbacks, and the Climate Benefits of Forests. Science, **320**, 1444–1449.

Bosch, F., 1997: Die Nutzung des Lebensraumes durch Reh (Capreolus capreolus Linné, 1758) und Damhirsch (Cervus dama Linné, 1758) im Naherholungsgebiet Kottenforst bei Bonn. Zeitschrift für Jagdwissenschaft, **43**, 15–23.

Buras, A., Rammig, A. & Zang, C.S., 2019: Quantifying impacts of the drought 2018 on European ecosystems in comparison to 2003. Biogeosciences Discussions, 1–23.

Chávez, R.O., Estay, S.A. & Riquelme, C.G., 2017: npphen: Vegetation Phenological Cycle and Anomaly Detection using Remote Sensing Data. https://CRAN.R-project.org/package=npphen.

Chávez, R.O., Rocco, R., Gutiérrez, Á.G., Dörner, M. & Estay, S.A., 2019: A Self-Calibrated Non-Parametric Time Series Analysis Approach for Assessing Insect Defoliation of Broad-Leaved Deciduous Nothofagus pumilio Forests. Remote Sensing, **11**, 204.

Duong, T., Wand, M., Chacon, J. & Gramacki, A., 2019: ks: Kernel Smoothing. https://CRAN.R-project.org/package=ks.

Estay, S.A. & Chávez, R.O., 2018: npphen: an R-package for non-parametric reconstruction of vegetation phenology and anomaly detection using remote sensing. bioRxiv, 301143.

Frantz, D., 2019: FORCE—Landsat + Sentinel-2 Analysis Ready Data and Beyond. Remote Sensing, **11**, 1124.

Frantz, D., Haß, E., Uhl, A., Stoffels, J. & Hill, J., 2018: Improvement of the Fmask algorithm for Sentinel-2 images: Separating clouds from bright surfaces based on parallax effects. Remote Sensing of Environment, **215**, 471–481.

Frantz, D., Röder, A., Stellmes, M. & Hill, J., 2016: An Operational Radiometric Landsat Preprocessing Framework for Large-Area Time Series Applications. IEEE Transactions on Geoscience and Remote Sensing, **54**, 3928–3943.

Gorelick, N., Hancher, M., Dixon, M., Ilyushchenko, S., Thau, D. & Moore, R., 2017: Google Earth Engine: Planetary-scale geospatial analysis for everyone. Remote Sensing of Environment, **202**, 18–27.

Hansen, M.C., Potapov, P.V., Moore, R., Hancher, M., Turubanova, S.A., Tyukavina, A., Thau, D., Stehman, S.V., Goetz, S.J., Loveland, T.R., Kommareddy, A., Egorov, A., Chini, L., Justice, C.O. & Townshend, J.R.G., 2013: High-Resolution Global Maps of 21st-Century Forest Cover Change. Science, **342**, 850–853.

HEALEY, S.P., COHEN, W.B., ZHIQIANG, Y. & KRANKINA, O.N., 2005: Comparison of Tasseled Cap-based Landsat data structures for use in forest disturbance detection. Remote Sensing of Environment, **97**, 301–310.

IMBERY, F., FRIEDRICH, K., KOPPE, C., JANSSEN, W., PFEIFROTH, U., DAßLER, J. & BISSOLLI, P., 2018: 2018 wärmster Sommer im Norden und Osten Deutschlands. https://www.dwd.de/DE/leistungen/besondereereignisse/temperatur/20180906_waermstersommer_nordenosten2018.html.

KOGAN, F.N., 1990: Remote sensing of weather impacts on vegetation in non-homogeneous areas. International Journal of Remote Sensing, **11**, 1405–1419.

MILLAR, C.I. & STEPHENSON, N.L., 2015: Temperate forest health in an era of emerging megadisturbance. Science, **349**, 823–826.

PAN, Y., BIRDSEY, R.A., FANG, J., HOUGHTON, R., KAUPPI, P.E., KURZ, W.A., PHILLIPS, O.L., SHVIDENKO, A., LEWIS, S.L., CANADELL, J.G., CIAIS, P., JACKSON, R.B., PACALA, S.W., MCGUIRE, A.D., PIAO, S., RAUTIAINEN, A., SITCH, S. & HAYES, D., 2011: A Large and Persistent Carbon Sink in the World's Forests. Science, **333**, 988–993.

R CORE TEAM, 2019: R: A language and Environment for Statistical Computing. Vienna, Austria. https://www.r-project.org/.

REINERMANN, S., GESSNER, U., ASAM, S., KUENZER, C. & DECH, S., 2019: The Effect of Droughts on Vegetation Condition in Germany: An Analysis Based on Two Decades of Satellite Earth Observation Time Series and Crop Yield Statistics. Remote Sensing, **11**, 1783.

SEIDL, R., THOM, D., KAUTZ, M., MARTIN-BENITO, D., PELTONIEMI, M., VACCHIANO, G., WILD, J., ASCOLI, D., PETR, M., HONKANIEMI, J., LEXER, M.J., TROTSIUK, V., MAIROTA, P., SVOBODA, M., FABRIKA, M., NAGEL, T.A. & REYER, C.P.O., 2017: Forest disturbances under climate change. Nature Climate Change, **7**, 395–402.

SENF, C., PFLUGMACHER, D., ZHIQIANG, Y., SEBALD, J., KNORN, J., NEUMANN, M., HOSTERT, P. & SEIDL, R., 2018: Canopy mortality has doubled in Europe's temperate forests over the last three decades. Nature Communications, **9**, 1–8.

SENF, C. & SEIDL, R., 2018: Natural disturbances are spatially diverse but temporally synchronized across temperate forest landscapes in Europe. Global Change Biology, **24**, 1201–1211.

WACHTER, H., 2009: Eichenheisterpflanzung – Eichensaat, ein Vergleich nach 100 Jahren. Allgemeine Forst- und Jagdzeitung, **180**, 177–184.

WAND, M.P. & JONES, M.C., 1995: Kernel smoothing, 1st ed. ed, Monographs on statistics and applied probability, Chapman & Hall, London & New York.

WULDER, M.A., HILKER, T., WHITE, J.C., COOPS, N.C., MASEK, J.G., PFLUGMACHER, D. & CREVIER, Y., 2015: Virtual constellations for global terrestrial monitoring. Remote Sensing of Environment, **170**, 62–76.

ZHANG, Y., PENG, C., LI, W., FANG, X., ZHANG, T., ZHU, Q., CHEN, H. & ZHAO, P., 2013: Monitoring and estimating drought-induced impacts on forest structure, growth, function, and ecosystem services using remote-sensing data: recent progress and future challenges. Environmental Reviews, **21**, 103–115.

ZHU, Z., WANG, S. & WOODCOCK, C.E., 2015: Improvement and expansion of the Fmask algorithm: cloud, cloud shadow, and snow detection for Landsats 4–7, 8, and Sentinel 2 images. Remote Sensing of Environment, **159**, 269–277.

ZHU, Z., WOODCOCK, C.E., OLOFSSON, P., 2012. Continuous monitoring of forest disturbance using all available Landsat imagery. Remote Sensing of Environment, **122**, 75–91.